Journal of Nuclear and Particle Physics 2014, 4(3): 100-115
DOI: 10.5923/j.jnpp.20140403.03

Mathematical Modeling for Pulsatile Flow of a Non-Newtonian Fluid with Heat and Mass Transfer in a Porous Medium between two Permeable Parallel Plates

Mohamed Y. Abou-zeid[1,2,*], Seham S. El-zahrani[1], Hesham M. Mansour[3]

[1]Department of Mathematics, Faculty of Science, Tabuk University, Tabuk, KSA
[2]Department of Mathematics, Faculty of Education, Ain Shams University, Roxy, Cairo, Egypt
[3]Department of Physics, Faculty of Science, Cairo University Giza, Egypt

Abstract The aim of the present work is to investigate the effect of mixed convection heat and mass transfer on pulsatile flow of a non-Newtonian fluid which is obeying the rheological equation of state due to Ree-Eyring's stress-strain relation. We take into consideration the porosity of medium and a uniform magnetic field. The flow is assumed to be between two permeable vertical plates. The equations of momentum, energy and concentration have been solved by using Lightill method. The velocity, temperature and concentration distributions are obtained. The effects of various parameters of the problem on these distributions are presented and discussed.

Keywords Pulsatile flow, Non-Newtonian fluid, Heat and mass transfer

1. Introduction

The study of pulsating flows is of practical engineering importance. High speed (turbulent) pulsating flows occur in turbo machinery, rotor blade aerodynamics, reciprocating piston-driven flows, etc. Numerous experimental investigations were focused on fundamental studies of fully developed periodic pipe flows with sinusoidal varying pressure gradients (or flow rates). Low speed (laminar) pulsating flows were studied in order to analyze the flows through small pipes or in the blood circulation systems. Laminar flows are relatively simple for analytical (or numerical) analysis and are a natural choice to provide basic studies of fundamental hydrodynamic effects in pulsating flows [1]. Pulsatile flow has also recently found renewed significance in its application to MEMS microfluidic engineering applications [2]. A complete treatment of the fluid dynamics of steady and pulsatory flow with emphasis on basic mechanics, physics and applications can be seen in Ref. [3].

Several investigations on flow through stenosed artery have been carried out to evaluate the flow characteristics under steady and pulsatile flow conditions. Young and Tsai [4-5] studied the steady and unsteady flows across a stenosis experimentally (See also Siouffi et al. [6]). In fact, blood is a complex rheological mixture showing several non-Newtonian properties, shear-thinning, yield stress, stress relaxation etc. The rheological properties of fluid have important influences on wall shear stress, oscillatory shear index etc. So it is very important to address the significance of non-Newtonian models for the purpose of reliable hemodynamic modeling [7]. Blood may be considered as a Newtonian fluid for the flow within the heart and the aorta of the human cardiovascular system. For blood flow in smaller arteries of diameter 0.5mm, a simple rescaling of the Newtonian viscosity is sufficient to take account of non-Newtonian behavior of the blood. In particular situations blood may behave as a non-Newtonian fluid, even in large arteries, as reported in Nakamura and Sawada [8]. Under diseased conditions, blood exhibits remarkable non-Newtonian properties. Eldabe et al. [9-10] studied pulsatile magneto hydrodynamic viscoelastic flow through a channel bounded by two permeable parallel plates and the effect of couple stresses on pulsatile hydro magnetic poiseuille flow.

The flow through porous media has attracted considerable research activity in recent years because of its important applications notably in the flow of oil through porous rock, the extraction of energy from the geothermal regions, the evaluation of the capability of heat-removal from particulate nuclear fuel debris that may result from a hypothetical accident in a nuclear reactor, the filteration of solids from liquids, flow of ion-exchange beds, drug permeation through human skin, chemical reactors for economical separation or purification of mixtures and so on [11]. Flow through porous

* Corresponding author:
master_math2003@yahoo.com (Mohamed Y. Abou-zeid)
Published online at http://journal.sapub.org/jnpp

media is very prevalent in nature, and therefore the study of flow through a porous medium has become of principle interest in many engineering applications. Thermal and solutal transport by fluid flowing through a porous matrix is a phenomenon of great interest from the theory and application point of view. Heat transfer in the case of homogenous fluid-saturated porous media has been studied in relation to different applications like dynamic of hot underground springs, terrestrial heat flow through aquifer, hot fluid and ignition front displacements in reservoir engineering, heat exchange between soil and atmosphere and heat exchanges with fluidized beds. Mass transfer in isothermal condition has been studied with applications to problems of mixing of fresh and salt water in a quifers, spreading of solutes in fluidized beds and crystal washers, salt leaching in soils, etc. Prevention of salt dissolution into the lake waters near the sea shores has become a serious and interesting problem of research [12].

Verma et al. [13] studied the pulsatile blood flow of a micro deformable fluid. A mathematical model for the study of blood flow through a channel with permeable walls of finite width is discussed by Mishra and Ghosh [14]. Vajravelu et al. [15] studied the pulsatile flow of a viscous incompressible Newtonian fluid between permeable beds. Lalit and Narayanan [16] discussed the analysis of pulsatile flow and its role on particle removal from surfaces. The pulsatile flow of blood through a mild stenosed artery under periodic body acceleration is investigated in this theoretical analysis by Mallik et. al. [17]. The problem of pulsatile flow of MHD non-Newtonian fluid obeying power law model with convective heat transfer through a non-Darcy porous medium between two coaxial cylinders is studied by Abou-zeid [18]. Shawky [19] studied the flow due to the pulsatile pressure gradient of dusty non-Newtonian fluid obeying Eyring-Powell model with heat transfer in a channel in the presence of external magnetic field.

The main idea of the present work is to study the mathematical analysis of a non-Newtonian fluid flow with heat and mass transfer. The flow analysis is developed through a porous media and between two vertical permeable parallel plates, in the presence of a normal magnetic field. Analytical solutions for the momentum, energy and concentration equations have been obtained under the assumption that the pulsatile flow is a linear combination of the steady part and the oscillatory part. Also, we show the relation between the different parameters of the flow and the external forces. Numerical solutions are obtained for different values of The parameters Re , k_0 , Ps , P_0 , Da , M , G_T , G_C , Pr , Sr , Sc , ω and t.

2. Mathematical Analysis

We consider the unsteady flow with heat and mass transfer of a viscous, incompressible, and electrically conducting non-Newtonian fluid (biviscosity fluid) in a porous medium between two permeable vertical parallel plates situated at $y = 0$ and $y = h$, under the action of the fluid gradient. The coordinates system used is shown in Fig. 1. The x- axis is taken in the direction of the flow and the y- axis is taken normal to the plates. We assume that a uniform magnetic field B_0 is acting along the y- axis. The fluid is being injected into the wall through $y = 0$ and is being sucked through $y = h$ with uniform velocity V_0.

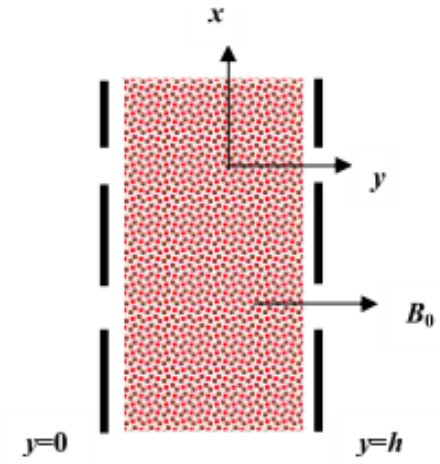

Figure 1. The coordinate system used

The governing equations used in this problem can be written as follows:

Continuity equation

$$\frac{d\rho}{dt} + \rho V_{i,i} = 0\,, \tag{1}$$

Momentum equation

$$\rho\left(\frac{\partial \underline{V}}{\partial t} + \underline{V}.\nabla\underline{V}\right) = -\nabla P + \nabla\cdot\underline{\tau} - \frac{\mu_f}{k_p}\underline{V} + \underline{J}\times\underline{B} + \underline{F} \tag{2}$$

Temperature equation

$$\frac{dT}{dt} = k_T\nabla^2 T\ , \tag{3}$$

Concentration equation

$$\frac{dC}{dt} = D_m\nabla^2 C + \frac{D_m K_T}{T_m}\nabla^2 T\,, \tag{4}$$

Nomenclature

a and b	Characteristics of Eyring-Powell model	R_e	Reynolds number $= \frac{hV_0}{\nu_f}$
$\underline{B}$	Total magnetic field	S_c	Schmidt number $= \frac{hV_0}{D_m}$
$B_{0\backslash}$	Uniform magnetic field		
C	Concentration of the species	S_r	Soret number $= \frac{D_m k_T (T_1 - T_2)}{hV_0 T_m (C_1 - C_2)}$
C_E	Ergun constant	t	Time
C_p	Specific heat at constant pressure	T	Temperature of the fluid
C_s	Concentration susceptibility	T_m	The mean temperature
Da	Darcy number $= \frac{V_0 k_p}{\nu_f h}$	V_0	the velocity of the suction or injection at the walls
D	Coefficient of mass diffusivity	$\underline{V}$	Velocity vector = (u, v, 0)
$\underline{F}$	The external body force		
G_T	Temperature Grashof number $= \frac{hg\beta^*(T - T_2)}{V_0^2}$	**Greek symbols**	
G_C	Concentration Grashof number $= \frac{hg\beta(C - C_2)}{V_0^2}$	β	The temperature coefficient of volumetric expansion
h	The distance between the two plates.	β^*	The mass coefficient of volumetric expansion
i	$\sqrt{-1}$	μ_f	Viscosity coefficient
$\underline{J}$	Current density	ω	Frequency of the oscillating plate
K_T	Thermal conductivity $= \frac{k_c}{\rho C_p}$	ρ	Density of the fluid
k_p	Constant permeability	σ	The electric conductivity
k_0	The parameter of the non-Newtonian fluid $= \frac{1}{ab\mu_f}$	$\underline{\tau}$	Stress tensor of the fluid.
M	Magnetic parameter $= \frac{\sigma B_0^2 h}{\rho V_0}$	**Superscripts and subscripts**	
P	Fluid pressure	1	Plate condition at y=0
P_0	The amplitude of the pulsation	2	Plate condition at y=h
P_s	The steady component of the pressure gradient	s	Steady component
		o	Oscillatory component
P_r	Prandtl number $= \frac{\nu_f}{k_T}$		

The rheological equation of state for an isotropic and incompressible flow of a Ree-Eyring fluid can be written as

$$\tau_{ij} = \mu_f \frac{\partial V_i}{\partial x_j} + \frac{1}{a}\sinh^{-1}\left(\frac{1}{b}\frac{\partial V_i}{\partial x_j}\right) \tag{5}$$

Since $\sinh^{-1} x \approx x$ for $|x| \le 1$, then

$$\tau_{ij} = \mu_f (1 + k_0)\frac{\partial V_i}{\partial x_j}, \tag{6}$$

For ordinary Newtonian fluid k_0=0.

Since the two walls are infinite, all quantities are functions of y and *t* only. From equation (1), we get v=V_0. Equations (2), (3) and (4) reduce to

$$\frac{\partial u}{\partial t} + V_0 \frac{\partial u}{\partial y} + \frac{1}{\rho}\frac{\partial P}{\partial x} = \nu_f (1 + k_0)\frac{\partial^2 u}{\partial y^2} - \left(\frac{\sigma B_0^2}{\rho} - \frac{\nu_f}{k_p}\right)u - g\beta(T - T_2) - g\beta^*(C - C_2), \tag{7}$$

$$\frac{\partial T}{\partial t} + V_0 \frac{\partial T}{\partial y} = k_T \frac{\partial^2 T}{\partial y^2}, \tag{8}$$

$$\frac{\partial C}{\partial t} + V_0 \frac{\partial C}{\partial y} = D_m \frac{\partial^2 C}{\partial y^2} + D_m \frac{k_T}{T_m}\frac{\partial^2 T}{\partial y^2}. \tag{9}$$

The appropriate boundary conditions are

$$\left.\begin{array}{llllll} u = 0, & T = T_1 & \text{and} & C = C_1 & \text{at} & y = 0, \\ u = 0, & T = T_2 & \text{and} & C = C_2 & \text{at} & y = h, \end{array}\right\}, \tag{10}$$

Let us introduce the following dimensionless quantities as follows:

$$\left.\begin{array}{l} u^* = \dfrac{u}{V_0},\quad x^* = \dfrac{1}{h}x,\quad y^* = \dfrac{1}{h}y,\quad \omega^* = \dfrac{h}{V_0}\omega,\quad t^* = \dfrac{V_0}{h}t, \\ P^* = \dfrac{1}{\rho V_0^2}P,\quad T^* = \dfrac{T - T_2}{T_1 - T_2},\quad C^* = \dfrac{C - C_2}{C_1 - C_2}, \end{array}\right\}. \tag{11}$$

Hence, Equations (7), (8) and (9) may be written in dimensionless form after dropping the star mark.

$$\frac{\partial u}{\partial t} + \frac{\partial u}{\partial y} + \frac{\partial P}{\partial x} = \frac{1}{\mathrm{Re}}(1 + k_0)\frac{\partial^2 u}{\partial y^2} - \left(M + \frac{1}{Da}\right)u - G_T T - G_C C, \tag{12}$$

$$\frac{\partial T}{\partial t} + \frac{\partial T}{\partial y} = \frac{1}{\mathrm{Re}\,P_r}\frac{\partial^2 T}{\partial y^2}, \tag{13}$$

$$\frac{\partial C}{\partial t} + \frac{\partial C}{\partial y} = \frac{1}{S_c}\frac{\partial^2 C}{\partial y^2} + S_r \frac{\partial^2 T}{\partial y^2}, \tag{14}$$

3. Method of Solution

For pulsation pressure gradient, let

$$-\frac{\partial P}{\partial x} = \left(\frac{\partial P}{\partial x}\right)_s + \left(\frac{\partial P}{\partial x}\right)_0 e^{i\omega t}, \tag{15}$$

Using Lightill method [20], the system of partial differential equations can be transformed into ordinary differential equations.

$$\left.\begin{aligned} u &= u_s + u_o e^{i\omega t}, \\ T &= T_s + T_o e^{i\omega t}, \\ C &= C_s + C_o e^{i\omega t} \end{aligned}\right\}. \tag{16}$$

Substituting from Eq's (16) and (17) in Eq's (12), (13) and (14) and equating the like terms on both sides, we get the following system equations:

$$\frac{1}{\mathrm{Re}}(1+k_0)\frac{d^2u_s}{dy^2} - \frac{du_s}{dy} - \left(M + \frac{1}{Da}\right)u_s - G_T\,T_s - G_C\,C_s = -\left(\frac{\partial P}{\partial x}\right)_s, \tag{17}$$

$$\frac{1}{\mathrm{Re}}(1+k_0)\frac{d^2u_o}{dy^2} - \frac{du_o}{dy} - \left(M + \frac{1}{Da} + i\,\omega\right)u_o - G_T\,T_o - G_C\,C_o = -\left(\frac{\partial P}{\partial x}\right)_o, \tag{18}$$

$$\frac{1}{\mathrm{Re}\,P_r}\frac{d^2T_s}{dy^2} - \frac{dT_s}{dy} = 0, \tag{19}$$

$$\frac{1}{R_e P_r}\frac{d^2T_o}{dy^2} - \frac{dT_o}{dy} - i\omega T_o = 0, \tag{20}$$

$$\frac{1}{S_c}\frac{d^2C_s}{dy^2} + S_r\frac{d^2T_s}{dy^2} - \frac{dC_s}{dy} = 0, \tag{21}$$

$$\frac{1}{S_c}\frac{d^2C_o}{dy^2} + S_r\frac{d^2T_o}{dy^2} - \frac{dC_o}{dy} - i\omega C_o = 0. \tag{22}$$

The dimensionless boundary conditions are

$$\left.\begin{aligned} &u_s = 0,\ u_o = 0,\ T_s = 1,\ T_o = 0,\ C_s = 1,\ C_o = 0 \quad \text{at } y = 0 \\ &u_s = 0,\ u_o = 0,\ T_s = T_o = 0,\ C_s = C_o = 0 \quad \text{at } y = 1 \end{aligned}\right\}. \tag{23}$$

The solutions of the equation (17) $\rightarrow$ (22) with boundary conditions (23) are

$$\begin{aligned} u = {} & a_{23}\,e^{a_{32}y} + a_{25}\,e^{a_{33}y} + a_{26}\,e^{a_{34}y} + a_{27}\,e^{a_{35}y} + a_{28}\,e^{a_{36}y} + a_{29}\,e^{a_{37}y} + \\ & a_{41}\,e^{a_{30}y} + a_{42}\,e^{a_{24}y} + \left(a_{43} + a_{44}\,e^{a_{12}y} + a_{45}\,e^{a_{10}y}\right)e^{i\omega t}, \end{aligned} \tag{24}$$

$$T = a_{13}\,e^{-a_3 y} + a_{14}\ , \tag{25}$$

$$C = a_{16}\,e^{-a_3 y} + a_{17}\,e^{-a_4 y} + a_{18}\ , \tag{26}$$

where $a_1 \rightarrow a_{45}$ are defined in the appendix.

4. Numerical Results and Discussion

The systems of equations that govern the non-Newtonian fluid between two vertical parallel plates are solved analytically. The formulas for velocity, temperature and concentration distributions are obtained. In order to get a physical understanding of the problem and for the purpose of discussing the results, numerical calculations have been performed to obtain the velocity, temperature and concentration. The velocity , temperature and concentration distributions are calculated for different values of Re , k_0 , P_s , P_0 , Da , M , G_T , G_C , Pr , Sr , Sc , ω and t in figures 2 - 20.

The effects of the physical parameters on the velocity distribution are shown in figures 2 - 13. In these figures the velocity distribution u is plotted versus the coordinate y. Figures 2 and 3, illustrate the effects of the parameter of the non-Newtonian fluid k_0 and Reynolds number Re respectively. It is found that the velocity increases with increasing Re, but it decreases with

increasing k0. We also noted that the velocity u increases with y till a definite value y = y0 (represents the maximum u) and it decreases afterwards. This maximum value of u increases by increasing Re while it decreases by increasing k_0. Shawky [19] showed that the velocity increases with the increase of Reynolds number. The effect of the magnetic parameter M on the velocity is shown in figure 4, and it is shown that the velocity u increases by increasing M in the range of y shown in the figure, and also, the velocity increases with y, till a maximum value (at a finite value of y : $y = y_0$) after which it decreases. It is clear that the maximum of u increases by increasing M and this also occurs at another value $y > y_0$. The variation of u with y for different values of Soret number Sr is drawn in Fig. 5. It is observed that the behavior of the curves is the same as that obtained in Fig. 4. The obtained curves are very close to those obtained in Fig. 4, and they coincide when $0 \le y \le 0.1$, and afterwards. u increases by increasing Sr.

In figures 6 and 7, the graphs of the velocity of the fluid have been drawn against y for different values of Ps and P_0, respectively. It is noticed that the behavior of the curves are the same as that obtained in Fig. 3.The effects of Darcy number Da and Prandtl number Pr on the velocity are elucidated in figures 8 and 9, respectively. It reveals that the velocity increases with increasing Pr, but it decreases with increasing Da. Figures 10 and 11, show the distribution of the velocity for various values of the temperature Grashof number G_T and concentration Grashof number G_C, Respectively. It is obvious that the velocity increases with the increase of both G_T and G_C. Also, the velocity increases with y, till a maximum value (at a finite value of y : $y = y_0$) after which it decreases.

The variations of the velocity distribution versus the coordinate y for various values of Schmidt number Sc is displayed in Fig. 12. The graphical results of Fig. 12 show that the velocity of fluid increases as Sc increases. While for $0.7 \le y \le 1$, near the right plate, the velocity decreases with the increase of Sc. The distributions of u within the coordinate y for various values of the time t and the frequency of the oscillating plate ω are exhibited in Figs. 13 and 14, respectively. From these figures, we observed that the effect of t and ω on u is opposite to the effect of Sc on u illustrated in Fig. 12, with the only difference that the obtained curves are very close to those obtained in Fig. 12.

The effects of Prandtl number Pr and Reynolds number Re on the temperature distribution T are indicated graphically in figures 15 and 16. In these figures, we observe that the temperature distribution increases with the increase of both Re and Pr. Also, the obtained curves in Fig. 16 are very close to those obtained in Fig. 15. The results in Fig. 15 and 16 are in agreement with those obtained by Shawky [19].

Figs. 17 and 18 show the behavior of the concentration C with the coordinate y for different values of Prandtl number Pr and Soret number Sr respectively. It is found that the effects of both Pr and Sr are to increase the concentration. Also, both Pr and Sr affect the relation between C and y. This relation is approximately linear at small values of Pr and Sr. In Figs. 19 and 20, the effects of Reynolds number Re and Schmidt number Sc on the concentration C respectively are presented. It is observed that the effect of Re and Sc on C is similar to the effect of Pr and Sr on C.

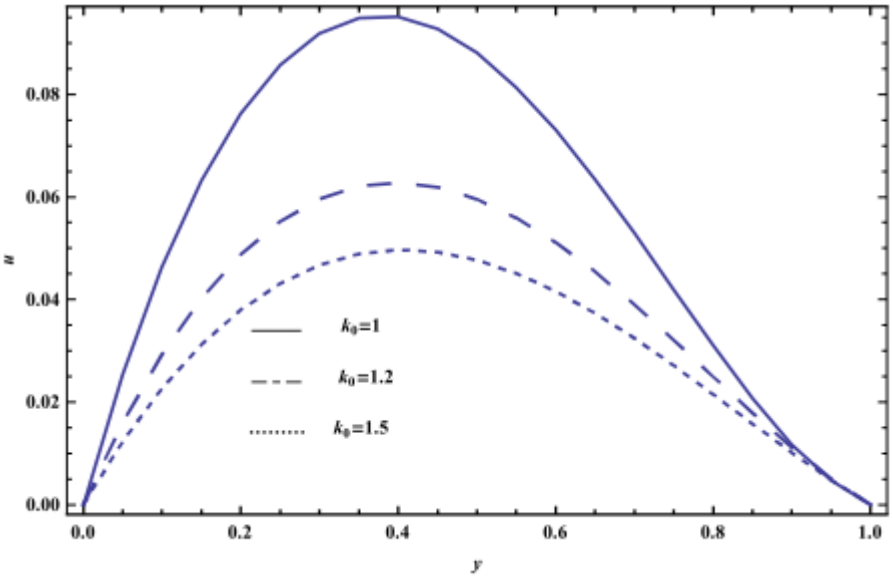

Figure 2. The velocity distribution is plotted versus y, for different values of k_0 and for a system which has the particular values Re =1.6, Da=0.5, M=3, Ps=2.5, P_0=0.5, ω=π/4, Pr=1, G_T=3.5, G_C=1.5, Sc=1.5, Sr=1, t=0.5

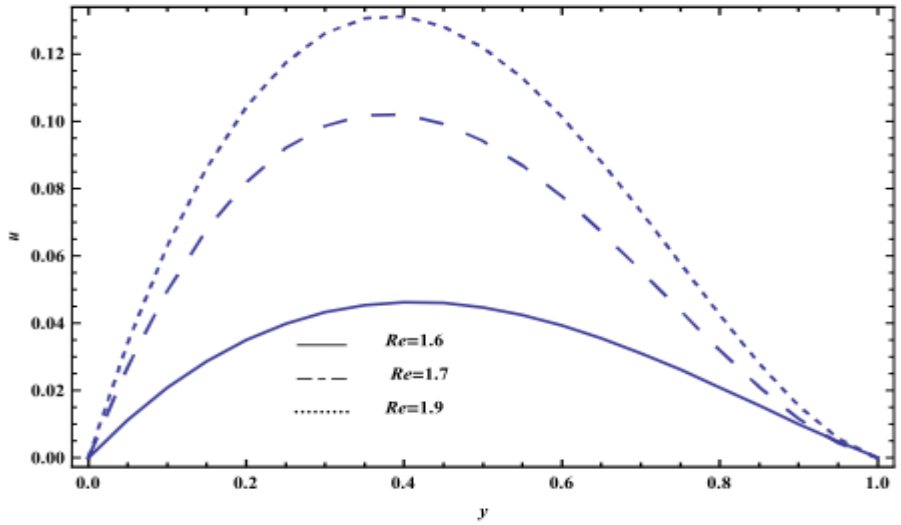

Figure 3. The velocity distribution is plotted versus y, for different values of Re and for a system which has the particular values k_0=1.5, Da=0.5, M=3, Ps=2.5, P_0=0.5, ω=π/4, Pr=1, G_T=3.5, G_C=1.5, Sc=1.5, Sr=1, t=0.5

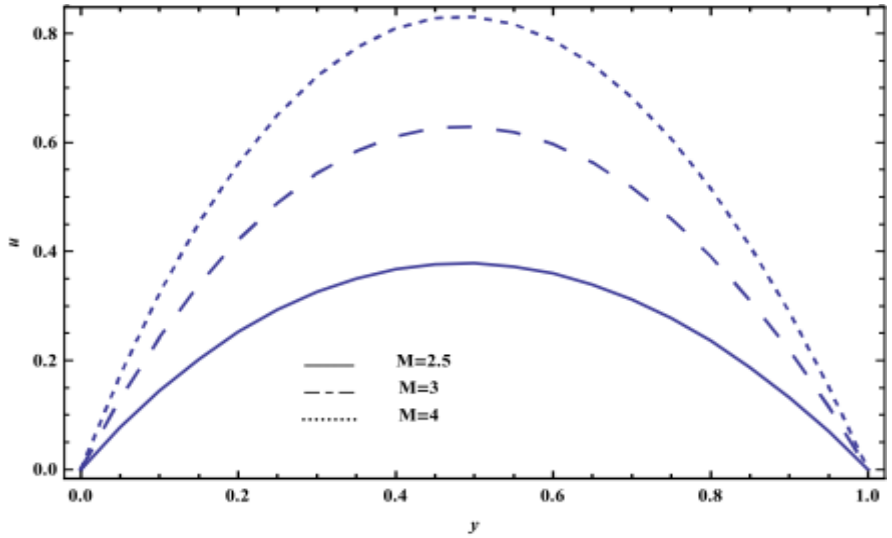

Figure 4. The velocity distribution is plotted versus y, for different values of M and for a system which has the particular values k_0=1.5, Re =1.6, Da=0.5, Ps=2.5, P_0=0.5, ω=π/4, Pr=1, G_T=3.5, G_C=1.5, Sc=1.5, Sr=1, t=0.5

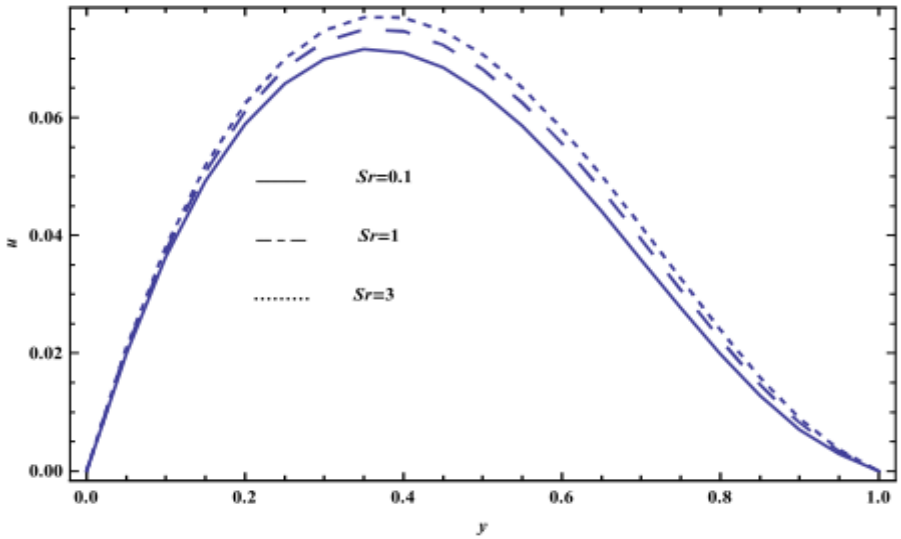

Figure 5. The velocity distribution is plotted versus y, for different values of Sr and for a system which has the particular values k_0=1.5, Re =1.6, Da=0.5, M=3, Ps=2.5, P_0=0.5, ω=π/4, Pr=1, G_T=3.5, G_C=1.5, Sc=1.5, t=0.5

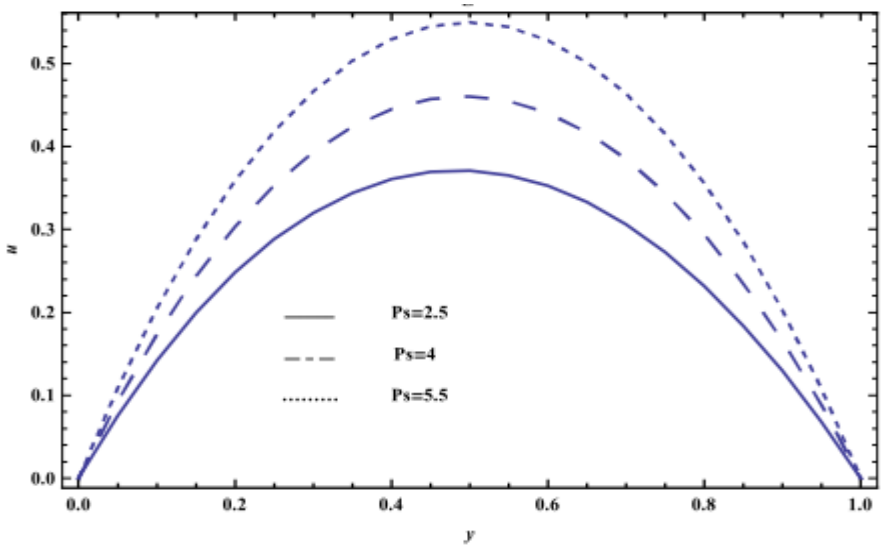

Figure 6. The velocity distribution is plotted versus y, for different values of Ps and for a system which has the particular values k_0=1.5, Re =1.6, Da=0.5, M=3, P_0=0.5, ω=π/4, Pr=1, G_T=3.5, G_C=1.5, Sc=1.5, Sr=1, t=0.5

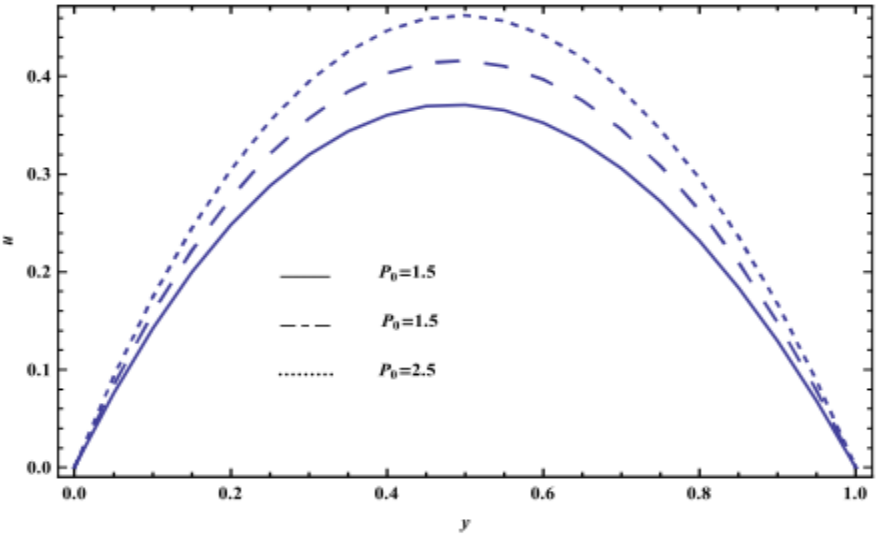

Figure 7. The velocity distribution is plotted versus y, for different values of P_0 and for a system which has the particular values k_0=1.5, Re =1.6, Da=0.5, M=3, Ps=2.5, ω=π/4, Pr=1, G_T=3.5, G_C=1.5, Sc=1.5, Sr=1, t=0.5

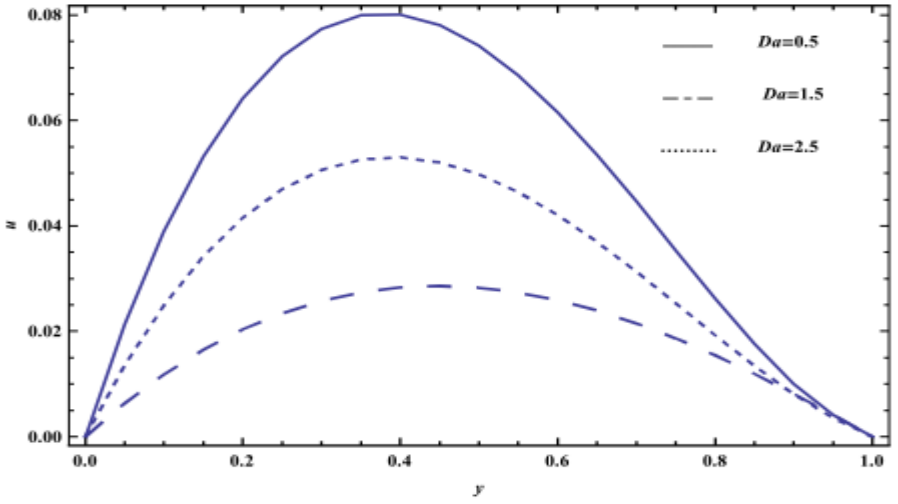

Figure 8. The velocity distribution is plotted versus y, for different values of Da and for a system which has the particular values k_0=1.5, Re =1.6, M=3, Ps=2.5, P_0=0.5, ω=π/4, Pr=1, G_T=3.5, G_C=1.5, Sc=1.5, Sr=1, t=0.5

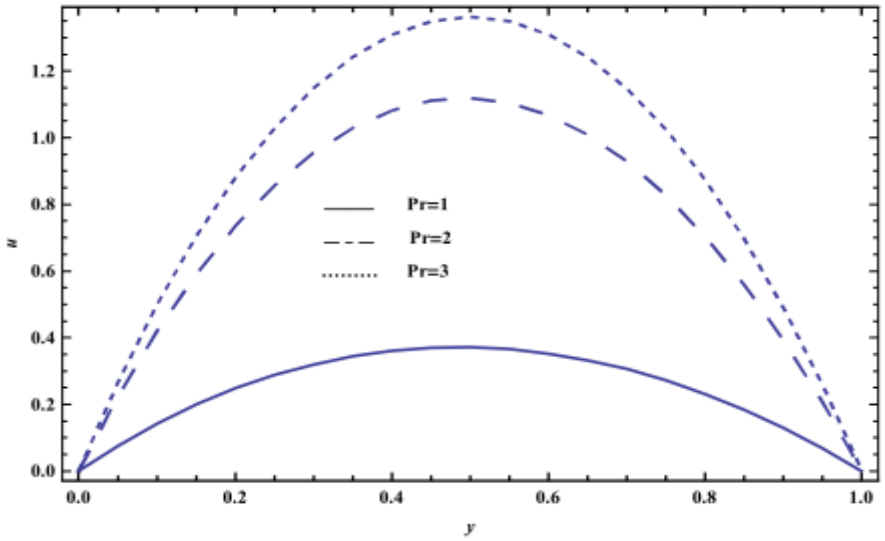

Figure 9. The velocity distribution is plotted versus y, for different values of Pr and for a system which has the particular values k_0=1.5, Re =1.6, Da=0.5, M=3, Ps=2.5, P_0=0.5, ω=π/4, G_T=3.5, G_C=1.5, Sc=1.5, Sr=1, t=0.5

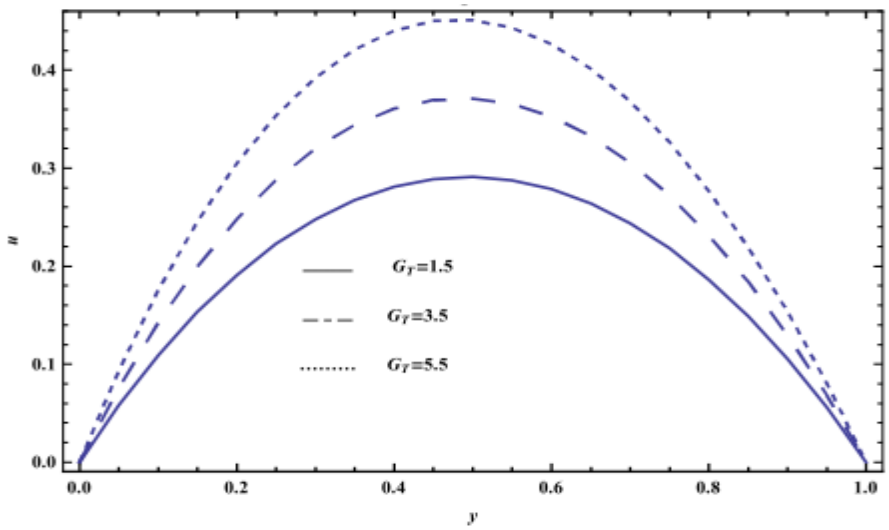

Figure 10. The velocity distribution is plotted versus y, for different values of G_T and for a system which has the particular values k_0=1.5, Re =1.6, Da=0.5, M=3, Ps=2.5, P_0=0.5, ω=π/4, Pr=1, G_C=1.5, Sc=1.5, Sr=1, t=0.5

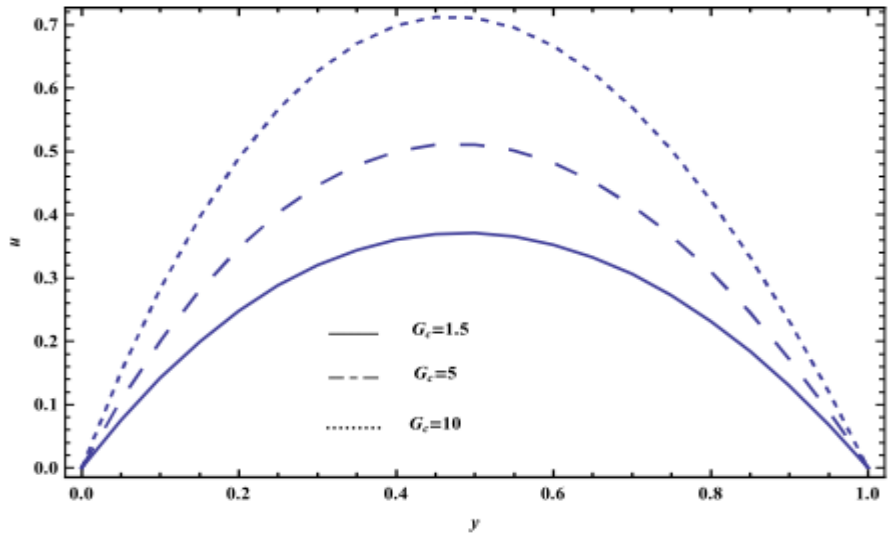

Figure 11. The velocity distribution is plotted versus y, for different values of G_C and for a system which has the particular values k_0=1.5, Re =1.6, Da=0.5, M=3, Ps=2.5, P_0=0.5, ω=π/4, Pr=1, G_T=3.5, Sc=1.5, Sr=1, t=0.5

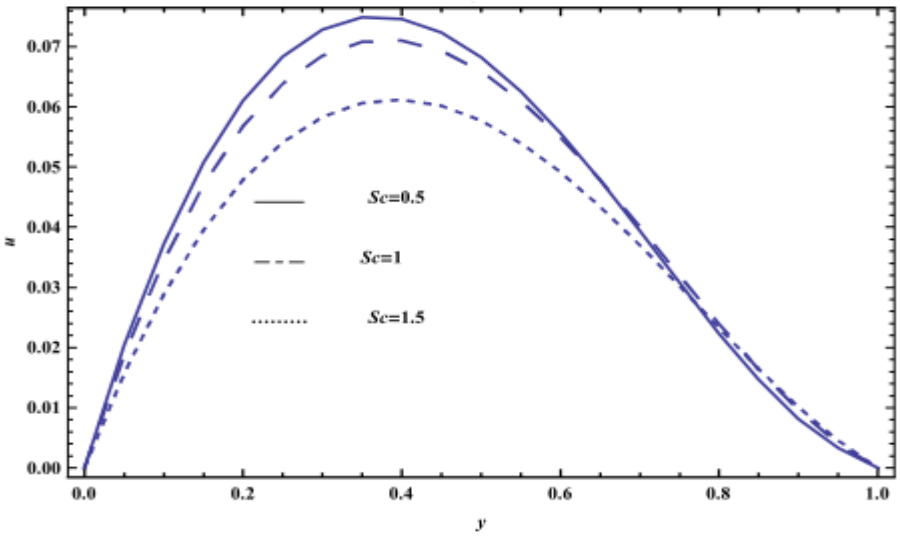

Figure 12. The velocity distribution is plotted versus y, for different values of Sc and for a system which has the particular values k_0=1.5, Re =1.6, Da=0.5, M=3, Ps=2.5, P_0=0.5, ω=π/4, Pr=1, G_T=3.5, G_C=1.5, Sr=1, t=0.5

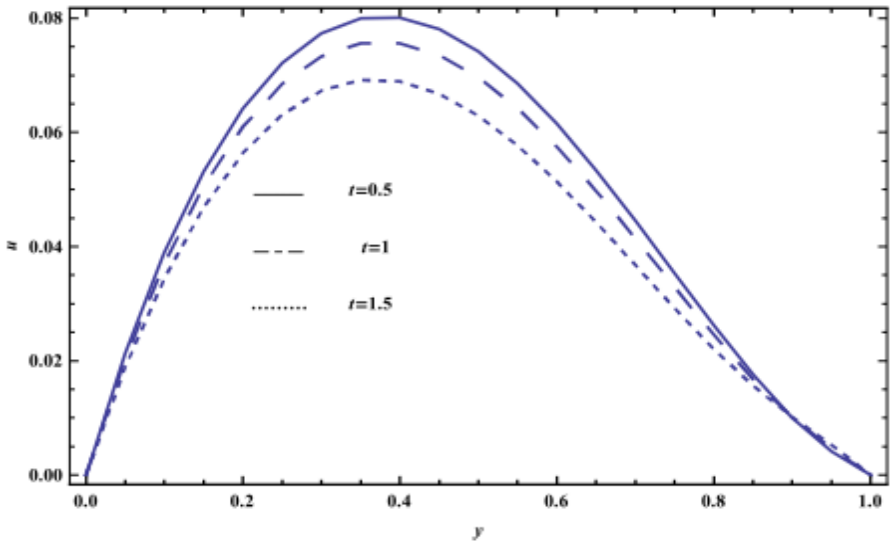

Figure 13. The velocity distribution is plotted versus y, for different values of t and for a system which has the particular values k_0=1.5, Re =1.6, Da=0.5, M=3, Ps=2.5, P_0=0.5, ω=π/4, Pr=1, G_T=3.5, G_C=1.5, Sc=1.5, Sr=1

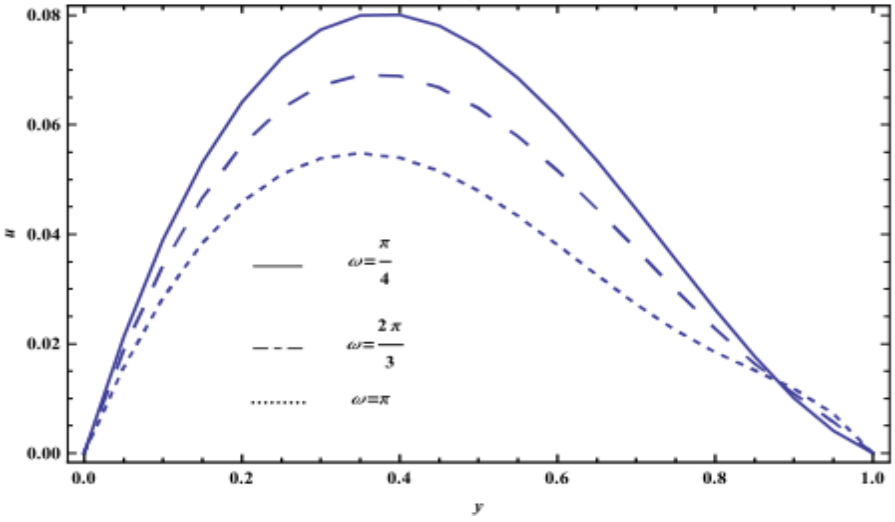

Figure 14. The velocity distribution is plotted versus y, for different values of ω and for a system which has the particular values k_0=1.5, Re =1.6, Da=0.5, M=3, Ps=2.5, P_0=0.5, Pr=1, G_T=3.5, G_C=1.5, Sc=1.5, Sr=1, t=0.5

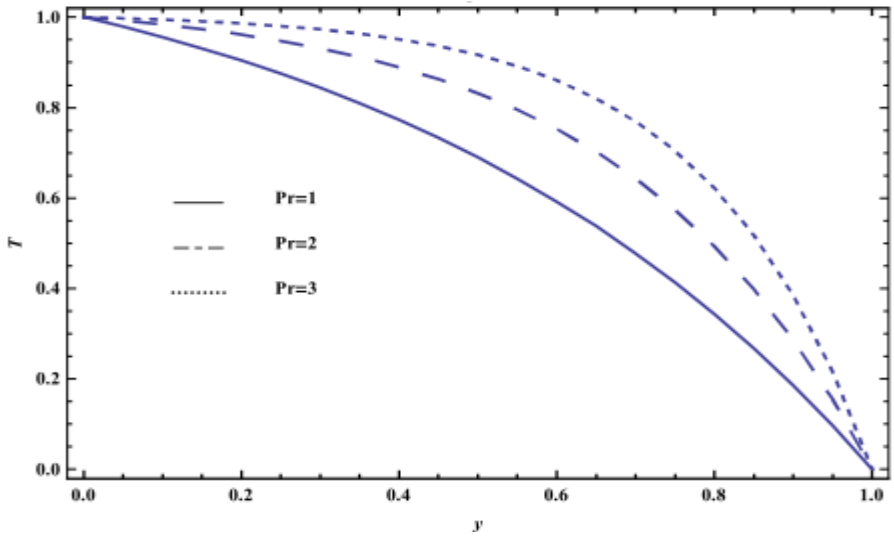

Figure 15. The temperature distribution is plotted versus y, for different values of Pr and for a system which has the particular values k_0=1.5, Re =1.6, Da=0.5, M=3, Ps=2.5, P_0=0.5, ω=π/4, G_T=3.5, G_C=1.5, Sc=1.5, Sr=1, t=0.5

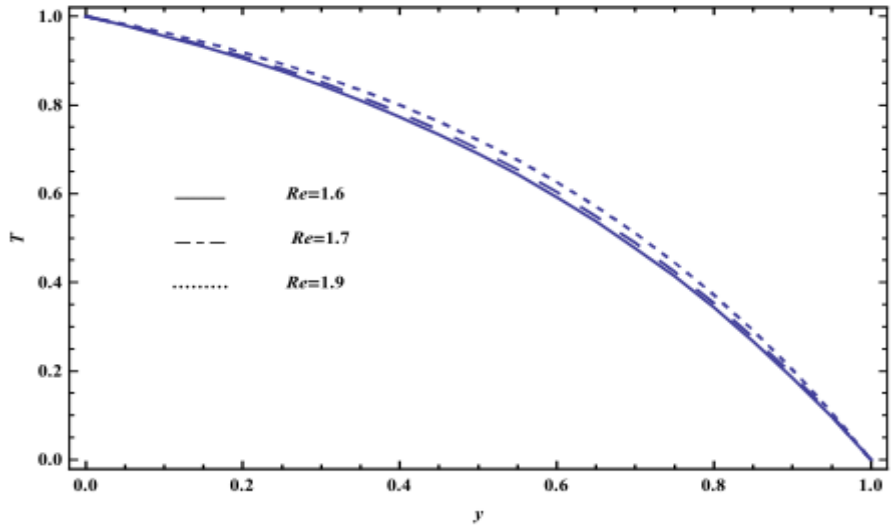

Figure 16. The temperature distribution is plotted versus y, for different values of Re and for a system which has the particular values k_0=1.5, Da=0.5, M=3, Ps=2.5, P_0=0.5, ω=π/4, Pr=1, G_T=3.5, G_C=1.5, Sc=1.5, Sr=1, t=0.5

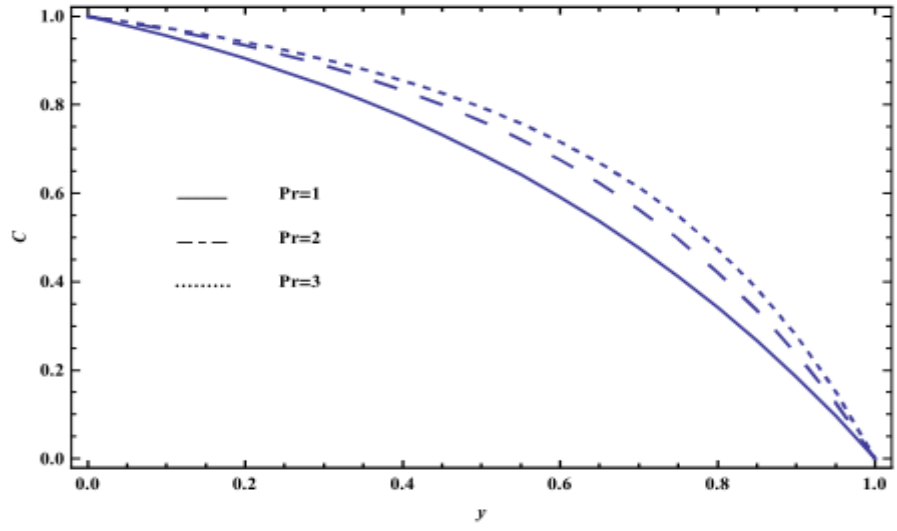

Figure 17. The concentration distribution is plotted versus y, for different values of Pr and for a system which has the particular values k_0=1.5, Re =1.6, Da=0.5, M=3, Ps=2.5, P_0=0.5, ω=π/4, G_T=3.5, G_C=1.5, Sc=1.5, Sr=1, t=0.5

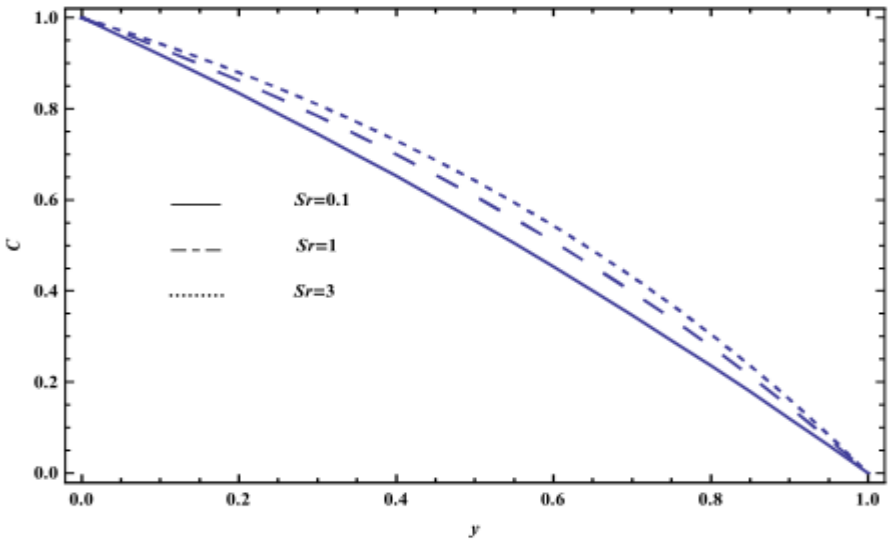

Figure 18. The concentration distribution is plotted versus y, for different values of Sr and for a system which has the particular values k_0=1.5, Re =1.6, Da=0.5, M=3, Ps=2.5, P_0=0.5, ω=π/4, Pr=1, G_T=3.5, G_C=1.5, Sc=1.5, t=0.5

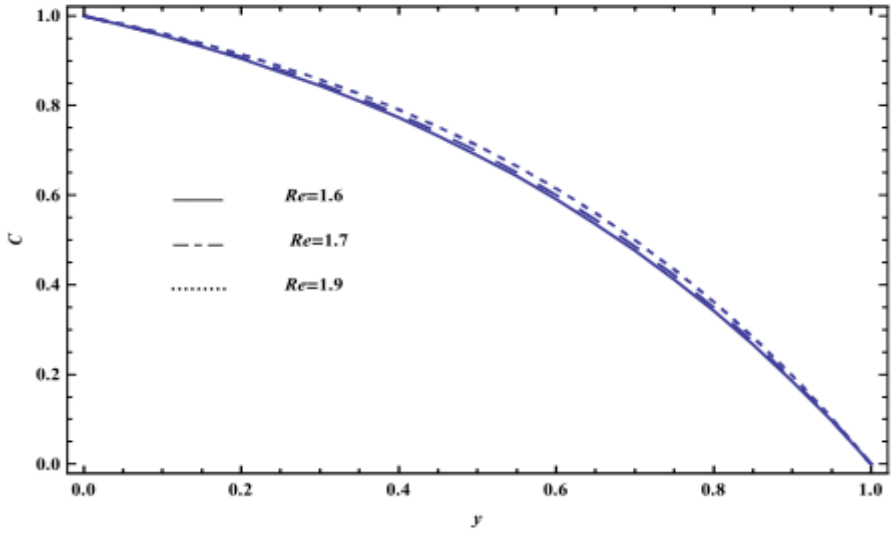

Figure 19. The concentration distribution is plotted versus y, for different values of Re and for a system which has the particular values k_0=1.5, Da=0.5, M=3, Ps=2.5, P_0=0.5, ω=π/4, Pr=1, G_T=3.5, G_C=1.5, Sc=1.5, Sr=1, t=0.5

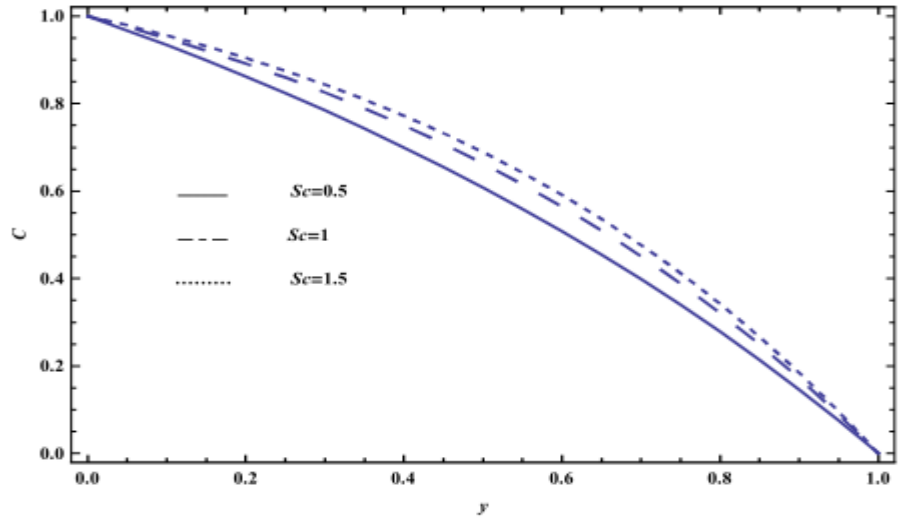

Figure 20. The concentration distribution is plotted versus y, for different values of Sc and for a system which has the particular values k_0=1.5, Re =1.6, Da=0.5, M=3, Ps=2.5, P_0=0.5, ω=π/4, Pr=1, G_T=3.5, G_C=1.5, Sr=1, t=0.5

5. Conclusions

In this paper, we have studied the problem of MHD unsteady flow with heat and mass transfer of non-Newtonian fluid which is obeying the rheological equation of state due to Ree-Eyring's stress-strain relation. The flow is through a uniform porous medium between two vertical permeable parallel plates in the presence of convective heat and mass transfer. The equations of momentum, energy and concentration are solved analytically by using Lightill method [20]. The velocity, temperature and concentration distributions are obtained. The effects of various physical parameters of the problems on these distributions are discussed and illustrated graphically through a set of figures. Hence, this paper deals with an important branch of fluid mechanics, which has many important applications in many fields, such as biology, medicine and chemistry and also in the space science e.g.:

1. The rheology of blood has received much study. Blood is rheologically complex on two counts: it is a suspension because erythrocytes with characteristic dimensions of several micrometers are present in excess of 40 % vol. and the suspension fluid itself exhibits non-Newtonian behavior because of the presence of high molecular-weight protein. The importance of rheological properties of other body fluids is now recognized. In particular, the rheological response of mucous in respiratory system of both infants and adults are an important factor for proper respiratory behavior. The lubricating action of synovial fluid in joints is likewise, strongly dependent on rheological properties [19].
2. For engineering purposes, one is more interested in the values of the velocity and heat transfer than in the shape of the velocity and temperature profiles. The results of this problem are of great interest in petroleum applications such as rotating machinery, lubrication technology, viscometry, computer storage devices, food processing, biochemical operations, transport in polymers and understanding and predicting blood flow properties in large arteries. The flow of the Petroleum through the Porous ground represents a good example of the motion of our fluid especially in the motion of the fluid in the earth's core. Also, there are many applications of this motion in many fields such Astrophysical, Plasma MHD, Metallurgical processes and Geophysical applications [18].

Appendices

$$a_1 = -\frac{\mathrm{Re}}{(1+k_0)},$$

$$a_2 = a_1\left(M + \frac{1}{Da}\right),$$

$$a_3 = -\mathrm{Re}\,\mathrm{Pr},$$

$$a_4 = -Sc,$$

$$a_5 = \frac{-1}{a_4},$$

$$a_6 = a_1\left(M + \frac{1}{Da} + i\,\omega\right),$$

$$a_7 = i\,\omega\,a_3,$$

$$a_8 = i\,\omega\,a_4,$$

$$a_9 = e^{\sqrt{a_1^2 - 4a_6}},$$

$$a_{10} = \frac{1}{2}\left(-a_1 + \sqrt{a_1^2 - 4a_6}\right),$$

$$a_{11} = \frac{1}{2}\left(a_1 + \sqrt{a_1^2 - 4a_6}\right),$$

$$a_{12} = \frac{1}{2}\left(-a_1 - \sqrt{a_1^2 - 4a_6}\right),$$

$$a_{13} = \frac{-1}{e^{-a_3} - 1} \ ,$$

$$a_{14} = \frac{e^{-a_3}}{e^{-a_3} - 1} \ ,$$

$$a_{15} = Sc\, Sr\, a_3{}^2\, a_{13} \ ,$$

$$a_{16} = \frac{\left(\frac{-a_{15}}{a_3\left(a_3 - a_4\right)}\right)}{\left(\frac{-a_{15}}{a_3\left(a_3 - a_4\right)}\right)\left(1 - e^{-a_3}\right) + a_5\left(1 - e^{-a_4}\right)} \ ,$$

$$a_{17} = \frac{a_5}{\left(\frac{-a_{15}}{a_3\left(a_3 - a_4\right)}\right)\left(1 - e^{-a_3}\right) + a_5\left(1 - e^{-a_4}\right)} \ ,$$

$$a_{18} = -\frac{\left(\frac{-a_{15}}{a_3\left(a_3 - a_4\right)}\right)e^{-a_3} + a_5\, e^{-a_4}}{\left(\frac{-a_{15}}{a_3\left(a_3 - a_4\right)}\right)\left(1 - e^{-a_3}\right) + a_5\left(1 - e^{-a_4}\right)} \ ,$$

$$a_{19} = -G_T\, a_{13} - G_C\, a_{16} \ ,$$

$$a_{20} = -G_C\, a_{17} \ ,$$

$$a_{21} = -G_T\, a_{14} - G_C\, a_{18} + \left(\frac{\partial P}{\partial x}\right)_s \ ,$$

$$a_{22} = -\frac{1}{2}\left(-a_1 + \sqrt{a_1{}^2 - 4a_2} + 2a_3 + 2a_4 \quad\right),$$

$$a_{23} = \frac{32}{a_{38}}\Big(a_1 a_2{}^2 a_{20} + \sqrt{a_1{}^2 - 4a_2}\; a_2{}^2 a_{20} - a_1{}^2 a_2 a_{20} a_3 - a_1\sqrt{a_1{}^2 - 4a_2}\; a_2 a_{20} a_3 +$$
$$a_1 a_{20} a_2 a_3{}^2 + a_{20}\sqrt{a_1{}^2 - 4a_2}\; a_2 a_3{}^2 - 2a_{20} a_2{}^2 a_4 + 2a_1 a_{20} a_2 a_3 a_4 - 2a_{20} a_2 a_3{}^2 a_4\Big) \ ,$$

$$a_{24} = \frac{1}{2}\left(-a_1 + \sqrt{a_1{}^2 - 4a_2}\right),$$

$$a_{25} = \frac{32}{a_{38}}\Big(a_1 a_{19} a_2{}^2 + a_{19}\sqrt{a_1{}^2 - 4a_2}\; a_2{}^2 - 2a_{19} a_2{}^2 a_3 - a_1{}^2 a_{19} a_2 a_4 + a_1 a_{19} a_2 a_4{}^2 -$$
$$a_1 a_{19}\sqrt{a_1{}^2 - 4a_2}\; a_2 a_4 + 2a_1 a_{19} a_2 a_3 a_4 + a_{19}\sqrt{a_1{}^2 - 4a_2}\; a_2\, a_4{}^2 - 2a_{19} a_2 a_3 a_4{}^2\Big) \ ,$$

$$a_{26} = \frac{32}{a_{38}}\Big(-a_1 a_2{}^2 a_{20} + \sqrt{a_1{}^2 - 4a_2}\; a_2{}^2 a_{20} + a_1{}^2 a_2 a_{20} a_3 - a_1\sqrt{a_1{}^2 - 4a_2}\; a_2 a_{20} a_3$$
$$- a_1 a_2 a_{20} a_3{}^2 + \sqrt{a_1{}^2 - 4a_2}\; a_2 a_{20} a_3{}^2 + 2a_2{}^2 a_{20} a_4 - 2a_1 a_2 a_{20} a_3 a_4 + 2a_2 a_{20} a_3{}^2 a_4\Big) \ ,$$

$$a_{27}=\frac{32}{a_{38}}\Big(a_1a_2{}^2a_{21}+\sqrt{a_1{}^2-4a_2}\,a_2{}^2a_{21}-a_1{}^2a_2a_{21}a_3-a_1\sqrt{a_1{}^2-4a_2}\,a_2a_{21}a_3$$
$$+a_1a_2a_{21}a_3{}^2+\sqrt{a_1{}^2-4a_2}\,a_2a_{21}a_3{}^2-a_1{}^2a_2a_{21}a_4-a_1\sqrt{a_1{}^2-4a_2}\,a_2a_{21}a_4+$$
$$a_1{}^3a_{21}a_3a_4+a_1{}^2\sqrt{a_1{}^2-4a_2}\,a_{21}a_3a_4-a_1{}^2a_{21}a_3{}^2a_4-a_1\sqrt{a_1{}^2-4a_2}\,a_{21}a_3{}^2a_4+\ ,$$
$$a_1a_2a_{21}a_4{}^2+\sqrt{a_1{}^2-4a_2}\,a_2a_{21}a_4{}^2-a_1{}^2a_{21}a_3a_4{}^2-a_1\sqrt{a_1{}^2-4a_2}\,a_{21}a_3a_4{}^2+$$
$$a_1a_{21}a_3{}^2a_4{}^2+\sqrt{a_1{}^2-4a_2}\,a_{21}a_3{}^2a_4{}^2\Big)$$

$$a_{28}=\frac{32}{a_{38}}\Big(-a_1a_{19}a_2{}^2+a_{19}\sqrt{a_1{}^2-4a_2}\,a_2{}^2+2a_{19}a_2{}^2a_3+a_1{}^2a_{19}a_2a_4-a_1a_{19}a_2a_4{}^2-$$
$$a_1a_{19}\sqrt{a_1{}^2-4a_2}\,a_2a_4-2a_1a_{19}a_2a_3a_4+a_{19}\sqrt{a_1{}^2-4a_2}\,a_2a_4{}^2+2a_{19}a_2a_3a_4{}^2\Big)\ ,$$

$$\alpha_{29}=\frac{32}{a_{38}}\Big(-a_1a_2{}^2a_{21}+\sqrt{a_1{}^2-4a_2}\,a_2{}^2a_{21}+a_1{}^2a_2a_{21}a_3-a_1\sqrt{a_1{}^2-4a_2}\,a_2a_{21}a_3$$
$$-a_1a_2a_{21}a_3{}^2+\sqrt{a_1{}^2-4a_2}\,a_2a_{21}a_3{}^2+a_1{}^2a_2a_{21}a_4-a_1\sqrt{a_1{}^2-4a_2}\,a_2a_{21}a_4-$$
$$a_1{}^3a_{21}a_3a_4+a_1{}^2\sqrt{a_1{}^2-4a_2}\,a_{21}a_3a_4+a_1{}^2a_{21}a_3{}^2a_4-a_1\sqrt{a_1{}^2-4a_2}\,a_{21}a_3{}^2a_4-\quad ,$$
$$a_1a_2a_{21}a_4{}^2+\sqrt{a_1{}^2-4a_2}\,a_2a_{21}a_4{}^2+a_1{}^2a_{21}a_3a_4{}^2-a_1\sqrt{a_1{}^2-4a_2}\,a_{21}$$
$$a_3a_4{}^2-a_1a_{21}a_3{}^2a_4{}^2+\sqrt{a_1{}^2-4a_2}\,a_{21}a_3{}^2a_4{}^2\Big)$$

$$a_{30}=\frac{1}{2}\Big(-a_1-\sqrt{a_1{}^2-4a_2}\Big),$$

$$a_{31}=\frac{1}{2}\Big(a_1+\sqrt{a_1{}^2-4a_2}-2a_3-2a_4\Big),$$

$$a_{32}=a_{24}+a_3+a_{22}\ ,$$

$$a_{33}=a_{24}+a_4+a_{22}\ ,$$

$$a_{34}=a_{30}+a_3+a_{31}\ ,$$

$$a_{35}=a_{24}+a_3+a_4+a_{22}\ ,$$

$$a_{36}=a_{30}+a_4+a_{31}\ ,$$

$$a_{37}=a_{30}+a_3+a_4+a_{31},$$

$$a_{38}=\Big(\Big(-a_1+\sqrt{a_1{}^2-4a_2}\Big)\Big(a_1+\sqrt{a_1{}^2-4a_2}\Big)\sqrt{a_1{}^2-4a_2}\Big(a_1+\sqrt{a_1{}^2-4a_2}-2a\Big)$$
$$\Big(-a_1+\sqrt{a_1{}^2-4a_2}+2a_3\Big)\Big(a_1+\sqrt{a_1{}^2-4a_2}-2a_4\Big)\Big(-a_1+\sqrt{a_1{}^2-4a_2}+2a_4\Big)\Big)\ ,$$

$$a_{39}=a_{23}+a_{25}+a_{26}+a_{27}+a_{28}+a_{29}\ ,$$

$$a_{40}=a_{23}\,e^{a_{32}}+a_{25}\,e^{a_{33}}+a_{26}\,e^{a_{34}}+a_{27}\,e^{a_{35}}+a_{28}\,e^{a_{36}}+a_{29}\,e^{a_{37}}\ ,$$

$$a_{41}=\frac{a_{40}-a_{39}\,e^{a_{24}}}{e^{a_{24}}-e^{a_{30}}}\ ,$$

$$a_{42} = -a_{39} - \left(\frac{a_{40} - a_{39}\, e^{a_{24}}}{e^{a_{24}} - e^{a_{30}}} \right),$$

$$a_{43} = \frac{\left(\frac{\partial P}{\partial x} \right)_o}{6},$$

$$a_{44} = -a_{43} \frac{\left(e^{a_{10}} - 1 \right)}{\left(e^{a_{10}} - e^{a_{12}} \right)},$$

$$a_{45} = a_{43} \left(-1 + \frac{\left(e^{a_{10}} - 1 \right)}{\left(e^{a_{10}} - e^{a_{12}} \right)} \right),$$

REFERENCES

[1] A. Yakhot, M. Arad, G. Ben-Dor, Numerical investigation of a laminar pulsating flow in a rectangular duct, Int. J. Numer. Meth. Fluids 29, (1999), 935-950

[2] F. Fedele, D. Hitt, R. D. Prabhu, Revisiting the stability of pulsatile pipe flow, Eur. J. Mech., B, Fluids, 24 (2005), 237–254.

[3] M. Zamir, The Physics of Pulsatile Flow, Springer-Verlag, New York, 2000.

[4] D. F. Young, F. Y. Tsai, Flow characteristics in models of arterial stenosis –I. Steady Flow, J. Biomechanics, 6, (1973), 395-410.

[5] D. F. Young, F. Y. Tsai, Flow characteristics in models of arterial stenosis –II. Unsteady Flow, J. Biomechanics, 6, (1973), 554-559.

[6] M. Siouffi, R. Pelisser, D. Farahifar, R. Rieu, The effect of unsteadiness on the flow through stenoses and Bifurcation, J.Biomechanics, 17, (1984), 299-315.

[7] M. S. Mandal, S. Mukhopadhyay, G. C. Layek, Pulsatile flow of shear-dependent fluid in a stenosed artery - Theoret. Appl. Mech., 39 (3), (2012). 209–231.

[8] M. Nakamura, T. Sawada, Numerical study on flow of non-Newtonian fluid through axi-symmetric stenosis, J .Biomech. Eng., 110, (1988), 247-26

[9] N. T. Eldabe, S. M. Elmohandis, Pulsatile magneto hydrodynamic viscoelastic flow through a channel bounded by two permeable parallel plates, J. Phys. Soc. Jpn., 64 (11), (1995), 4165.

[10] N. T. Eldabe, S. M. Elmohandis, Effect of couple stresses on pulsatile poiseuille flow, Fluid Dynamic Research 15 (1995), 313.

[11] P. Bitla, T. Kandala, V. Iyengar, Pulsating flow of an incompressible micro polar fluid between permeable beds, Nonlinear Analysis: Modeling and Control, 18 (4), (2013), 399–411.

[12] M. A. Abdelnaby, N. T. M. Eldabe and M. Y. Abou-zeid, Numerical study of pulsatile MHD non-Newtonian fluid flow with heat and mass transfer through a porous medium between two permeable parallel plates, Ind. J. Mech. Cont. & Math Sci, 1, (2006), 1-15.

[13] P. D. S. Verma, D. U. Singh, K. Singh, Pulsatile blood flow of a micro deformable fluid, Wear, 71, (1981), 333–346.

[14] J. C. Misra, S. K. Ghosh, A mathematical model for the study of blood flow through a channel with permeable walls, Acta Mech., 122, (1997), 137–153.

[15] K. Vajravelu, K. Ramesh, S. Sreenadh, P. U. Arunachalam, Pulsatile flow between permeable beds, Int. J. Non-Linear Mech., 38, (2003), 999–1005.

[16] L. Kumar, S. Narayanan, Analysis of pulsatile flow and its role on particle removal from surfaces, Chem. Eng. Sci., 65, (2010), 5582–5587.

[17] B. Mallik, S. Nanda, B. Das, D. Saha, D. S. Das, K. Paul, Pulsatile flow of casson fluid in mild stenosed artery with periodic body acceleration and slip condition, Sch. J. Eng. Tech., 1(1), (2013), 27-38.

[18] M. Y. Abou-zeid, Numerical solutions for heat generation effect on MHD pulsatile non-Newtonian fluid flow with convective heat transfer in a non-Darcian porous medium between two rotating cylinders, Bull. Cal. Math. J. 101, (2009), 531-55

[19] H. M. Shawky, Pulsatile flow with heat transfer of dusty magneto hydrodynamic Ree-Eyring fluid through a channel, Heat Mass Transfer, 45(10), (2009), 1261-1269.

[20] M. J. Lighthill, Introduction to Fourier analysis and generalized functions, Bull. Amer. Math. Soc., 65 (4), (1959), 248-249.